CHEMISTRY
A EUROPEAN JOURNAL

DOI: 10.1002/chem.200800674

Chemistry in Confining Reaction Fields with Special Emphasis on Nanoporous Materials

Sebastian Polarz* and Andreas Kuschel[a]

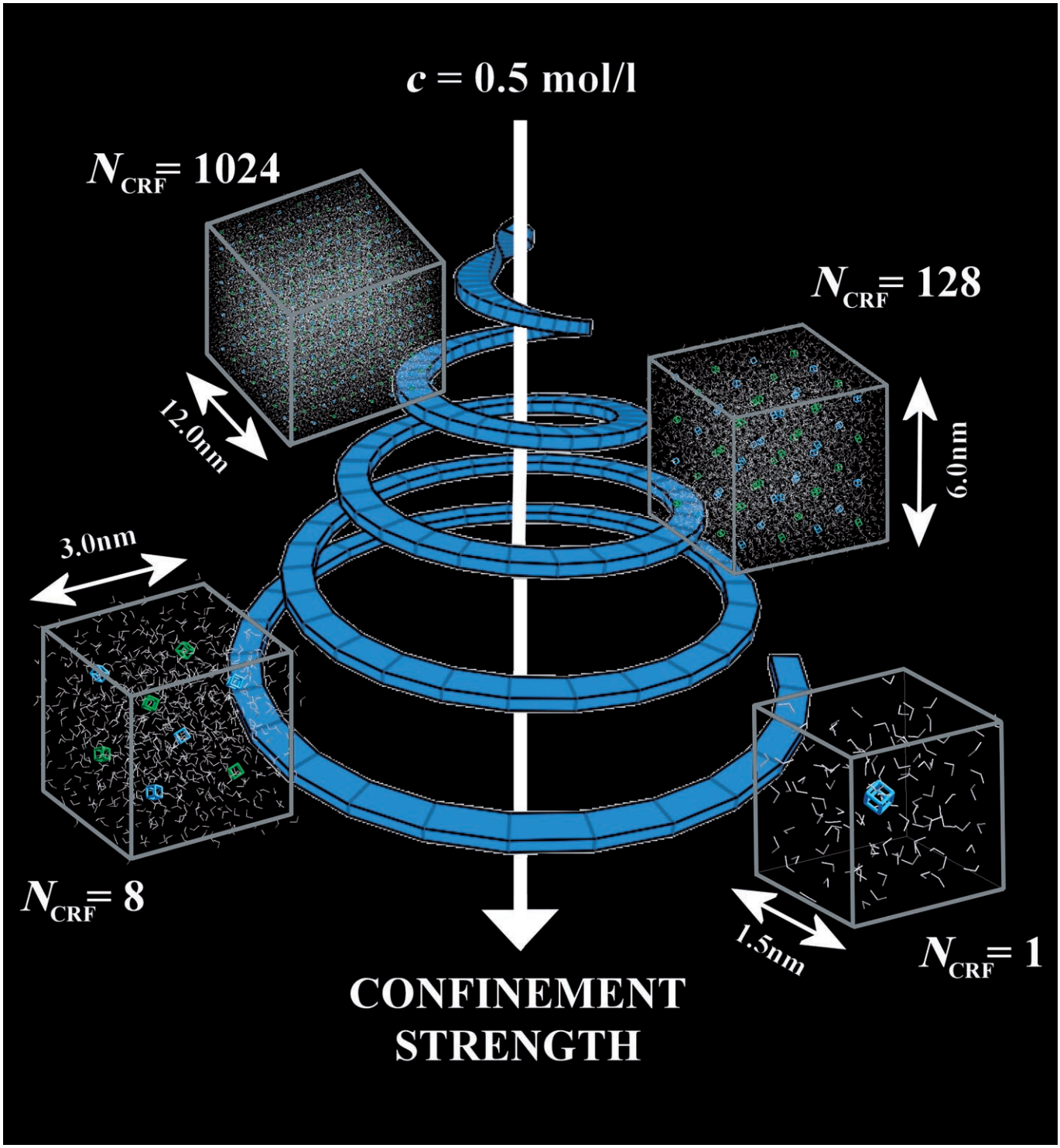

Abstract: The everyday routine of most chemists is dictated by large numbers. The chemical rules for ensembles of molar size ($N \approx N_A = 6.022 \times 10^{23}$) are well known and can be understood in most cases by using Boltzmann distribution. It is an interesting question how a small ensemble of a chemical system behaves and if it differs from the respective large-ensemble counterpart. The experimental approach presented in the current paper involves the division of a macroscopic volume into compartments that contain only a small number of reactants. The compartments represent the pores of tailor-made nanoporous materials.

Keywords: confinement effects · host–guest systems · mesoporous materials · nanochemistry · surface design

Introduction

One of the paramount paradigms in catalysis is that the catalyst affects only the rate of the respective conversion, whereas the equilibrium constant K is not altered. This is surely true. The catalyst forms a transitional conjunction with the reactants and vacates the conversion as it entered. The transitional states are represented by a sequence of reaction paths that are different to the noncatalysed case due to chemical bonding to the catalyst. These "new" reaction paths are associated with at least one lower activation barrier, leading to overall higher reaction rates $k_{r\rightarrow p}$ (r = reactants, p = products), but constant equilibrium $K = k_{r\rightarrow p}/k_{p\rightarrow r}$. In heterogeneous catalysis, solid-state or molecular type, catalytically active species are present at the interface of a solid material. As a consequence, the maximisation of interface becomes an important task. Porous materials or materials composed of small particles may exhibit a large surface area.[1] Ultimately, the catalyst itself might be produced in a porous form, or in the form of small particles. Alternatively, the catalyst can be immobilised on particles or on the internal surfaces of a porous support, metallocene polymerisation catalysts bound to silica particles or attached to mesoporous silica being nice examples.[2] Both subjects have already been extensively described in several excellent review articles.[3,4]

However, for chemical reactions occurring in the vicinity of solid surfaces a possibility exists that an additional factor influences the outcome of the reaction. Unlike in solution or gas phase, the reactants cannot move freely in 3D space anymore. In other words, the reacting system is restricted to a confining reaction field (CRF). It is an interesting idea to specify the strength of such a confinement by the mean curvature of a surface (H), which is defined by two orthogonal curvature radii [Eq. (1)].

$$H = 0.5\left(\frac{1}{\pm R_1} + \frac{1}{\pm R_2}\right) \quad (1)$$

The two principal curvatures can either be positive or negative, depending on if the surface is locally convex or concave. In the case of $H \geq 0$, the mobility of a molecule at the surface is only restricted due to geometric factors alone. The degree of confinement will be influenced mainly by the interaction between the reactants and the surface (see Scheme 1, i). A volume surrounded by an interface with negative curvature (Scheme 1, iii) is most effective regarding spatial restriction, more or less irrespective of the character of interaction (attractive or repulsive). Because the surface to volume ratio increases with increasing curvature, albeit its sign, it is reasonable to argue that the chemical and physical properties of the surface will gain further importance for large curvatures or small nanoscaled structures. Although we believe that consideration of the mean curvature is rather useful, it needs to be mentioned that nano-objects with rectangular shape, for instance nanocubes, also possess significant amounts of interface in relation to volume and might also represent interesting candidates as CRFs, although the interfaces themselves are not curved.

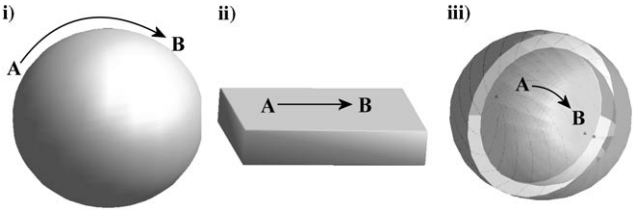

Scheme 1. Schematic representation indicating a chemical reaction proceeding from reactant A to product B in the vicinity of the surface of a system with i) positive curvature, $H > 0$ (i.e., a particle), ii) zero curvature (i.e., a flat surface) and iii) negative curvature, $H < 0$ (i.e., a pore).

In the current paper we are interested in the influence of CRFs on chemical processes impartial from a catalytic activity of the materials. However, it should be emphasised that confinement effects are likely to play a role in catalysed reactions occurring in the vicinity of surfaces.

A Gedanken Experiment—The Ideal Confining Reaction Field

Although Scheme 1 illustrates a purely geometrical construction, it is intuitive that surfaces with $H < 0$ lead to the separation of a particular volume. If this volume is small it

[a] Prof. Dr. S. Polarz, A. Kuschel
Department of Chemistry, University of Konstanz
78457 Konstanz (Germany)
Fax: (+49) 7531-884406
E-mail: sebastian.polarz@uni-konstanz.de

leads to a significant spatial restriction. Therefore, strong CRFs can be expected from porous materials with pore size (D_{pore}) of just a few nanometers (mesopores with 2 nm > D_{pore} > 50 nm, or micropores D_{pore} < 1 nm).[5] Alternatively, the interior of a small droplet, like in emulsions or micelles, represent promising CRFs.[6] Due to the arguments mentioned above, one important criterion for a good CRF is the ability to adjust the chemical and physical properties of the interface surrounding the confinement, indicated as hierarchy level I in Scheme 2. Such an adjustment can only be

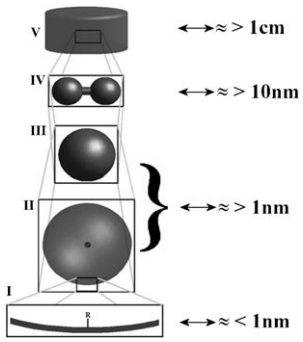

Scheme 2. Schematic representation indicating the hierarchy of requirements for confining reaction fields. Level I: properties of the confining interface; level II: CRF size; level III: CRF shape; level IV: CRF accessibility/connectivity; level V: macroscopic CRF assembly.

managed if one gains control over the functional groups attached to the confining surface. The next key factor is the option to generate CRFs with different dimensions of the order 1–20 nm and as monodisperse in size as possible (hierarchy level II in Scheme 2). The CRF volume (V_{CRF}), at given concentrations (c) of reactants, determines the size of the ensemble per CRF, as indicated in Equation (2), with N_A = Avogadro constant. Note that N_{CRF} considers only the number of potential reactants and not the total number of molecules per confinement, including solvent molecules.

$$N_{CRF} = c\left(\frac{\text{mol}}{\text{l}}\right) V_{CRF} N_A \qquad (2)$$

The shape of the CRF (hierarchy level III) is also of some interest as it allows us to investigate 3D confinements (spherical compartments), 2D confinements (cylindrical compartments) and 1D confinements (laminar compartments). A crucial, and to a certain degree contradictory, issue is the accessibility of a single CRF. An ideal CRF prevents any mass and energy transfer to or from the environment. If the CRF was an isolated pore, separated from the environment by a solid, robust wall, it would be extremely difficult to open, fill, empty, or re-seal it. Thus, it became impossible to study confined processes in porous solids. At least limited accessibility of pores is inevitable. Although there is no direct connection between micelles or emulsion droplets, they may not necessarily represent ideal CRFs with respect to criterion IV (Scheme 2). This is due to the high dynamics, fusion and fission of self-assembled soft-matter structures in solvents. However, there have been indications that under certain circumstances emulsion droplets are stable and do not exchange on a timescale of weeks.[7] Because it is so difficult to gain control over criterion IV it is important to take care that exchange processes taking place between the individual CRFs (for instance mass exchange by diffusion) proceed on a timescale significantly slower than the chemical processes for which confinement effects are to be studied. Finally, it can be experimentally very difficult to investigate one single compartment containing only a limited number of molecules. Therefore, it is profitable to have a large number of identical CRFs available that can be observed simultaneously. However, this creates the additional problem that we need to ensure that single CRFs are assembled in such a way that no additional volume accessible for the ongoing chemical processes is present.

In the following paragraphs it will be highlighted in how far nanoporous materials fulfil the mentioned requirements formulated for CRFs. Finally, some examples for chemistry in confining reaction fields are described.

The preparation of mesoporous materials with narrow pore-size distribution: Because a large number of excellent and comprehensive review articles have already been published on the preparation of mesoporous materials, only a very brief description about the synthesis of this class of materials is given here.[1,4,8] Porous materials in general can be generated from the combination of a cross-linking process forming an inorganic network and a template. If the template size is of the order of 2–50 nm, an attractive force between the template surface and the inorganic network exists, and if the crystallite size of the inorganic network is sufficiently small, the pore size will be in the meso-regime after template removal. The formation of inorganic oxides is most frequently achieved by sol–gel processing starting from alkoxide precursors. Due to the narrow pore-size distributions and the ordered pore systems, mesoporous materials originating from lyotropic phases as templates have gained enormous impact since 1992, when MCM-41 was reported, a silica material with ≈3 nm wide cylindrical pores aligned in a hexagonal fashion.[9,10] Another classical example is the so-called SBA-15 material, prepared from a lyotropic phase of an amphiphilic PEO-PPO-PEO (PEO = poly(ethylene oxide); PPO = poly(propylene oxide)) block copolymer (Pluronic) and $Si(OEt)_4$ in acidic solution.[11,12] The $Si(OEt)_4$ hydrolyses and polycondensates in the hydrophilic domains of the liquid crystal. In an ideal case, the pore system represents a 1:1 replica of the template structure.[13] In addition to the mesopores, it is known for many ordered mesoporous materials (OMMs) that they also possess a significant amount of micropores. For instance, the micropores in SBA-15 are caused by PEO chains from the block-copolymer template penetrating into silica network.[14] The micropores might represent an additional CRF system. However, because their volume is rather small in comparison to the mes-

opores, the confinement effect should be less significant with respect to the entire system restricted to pores. In the following, we will concentrate on silica OMMs as CRFs.

Hierarchical Features of Mesoporous Silica Materials as Prototypes for Confining Reaction Fields

Surface properties of mesoporous silica materials: Considering the preparation of mesoporous silica materials described briefly in the previous section, different approaches can be identified to influence the properties of the surfaces of the CRFs (hierarchy level I; Scheme 2). Functional groups R can be attached to the surfaces by post-synthetic modification, meaning that the porous material is prepared first and then treated with a functionalised compound reacting at the interfaces. An alternative, more direct approach is to use already functionalised precursors leading to a modified network composition and bringing the desired functional R groups to the surface. Good progress has been made on post-synthetic functionalisation, also known as grafting, for silica materials. Grafting is possible because silica prepared by sol–gel methods possesses reactive silanol groups (Si–OH) at the surfaces, even after calcination. Typically, the density of silanol groups in OMMs is of the order of 1–3 groups per nm^2.[15] Surface modification with pendant organic groups can be achieved by Si-O-Si bond formation by using suitable organosilanes. Both bond types, Si-O-Si and Si–C are chemically inert. They are stable in air up to 300 °C (for Si–C), sometimes even higher, and stable in acids (except Si-O-Si in hydrofluoric acid) and under moderate basic conditions. Suitable organosilanes are R_3SiCl (with R = an organic group) or alkoxide precursors $(R'O)_3$-SiR.[16,17] Many different systems have been prepared by using the grafting strategy; for example, relatively elementary surface modifications like attached alkyl or aminoalkyl groups. In the meantime, the development has gone much further, from very complex functions like surface-bound, catalytically active, transition-metal complexes—for instance the immobilisation of a bimetallic, ferrocene-containing, Pd-catalyst on mesoporous silica[18]—to sensors or biological active receptors,[19,20] to name only a few. However, there are certain disadvantages associated with the grafting technique. The pendant organic substituent and potential gelation of the surface modification agent leads to a decrease in pore size, or even complete closure of the pore. Depending on accessibility and density of Si–OH groups (see above), only a fraction of the silanols are modified. The composition of the materials has to be described as $(SiO_2)_{1-x}$•$(RSiO_{1.5})_x$ in which x can be as high as 20%; cases of only 5% modification have also been reported.[9,20] Thus, it is also very difficult to guarantee a homogeneous distribution of the organic groups along the pore surface.

The ability of the mentioned organoalkoxysilanes to form cross-linked organosilica gels can also be used as an advantage. The materials $RSiO_{1.5}$ obtained from the pure precursors $(R'O)_3SiR$ can be prepared in both a porous and non-porous form.[17,21] Unfortunately, the preparation of OMMs with a narrow pore-size distribution from organic liquid crystals as templates was not possible unless the organosilane is diluted with a source of pure silica: $(1-x)\,Si(OR)_4 + x\,(R'O)_3SiR \rightarrow (SiO_2)_{1-x}$•$(RSiO_{1.5})_x$. The described method became known as the co-condensation approach and was first applied to MCM-41-type materials in 1996.[22] However, there are many problems associated with the co-condensation method that arise from the inevitable dilution of the organosilica matrix with pure silica. It was only possible to derive a pore systems typical for OMMs from ≈25% or less of $(R'O)_3SiR$ used during the sol–gel process. The reason for this phenomenon is probably that the microphase separation into hydrophobic and hydrophilic domains leading to the lyotropic phase (the template) is hindered due to the stronger hydrophobic character induced by the pendant organic substituent in $(R'O)_3SiR$ and also its dipolar orientation. Furthermore, the organic substituent attached to the silicon atoms affects the hydrolysis kinetics of the Si-OR′ bonds in comparison to the tetraalkoxysilanes. In an extreme case, if the kinetics are significantly different, it might come to two, more or less independent, gel-formation steps. All three factors, enhanced hydrophobicity, limited degree of organic modification and changed gelation kinetics are negative factors with respect to a good homogeneity of the material and the surfaces.

The problems mentioned for grafting and co-condensation were solved when a new class of materials was introduced in 1999 by three independent groups: The so-called periodic mesoporous organosilica (PMO) materials.[23–25] The mesoporous materials were prepared by using silsesquioxane precursors possessing a bridging organic group R: $(R'O)_3Si$-R-$Si(OR')_3$. Interestingly, the bridged silsesquioxane precursors were known before the synthesis of OMMs.[26] It has to be emphasised, that for real PMOs the organosilane precursor is not further diluted with a precursor leading to pure SiO_2, as described in the co-condensation case. The enhanced hydrophobicity of the organic substituent R is compensated by the two silicic acid building blocks arranged in such a way that a weaker dipole results in comparison to $(R'O)_3SiR$. This allows the use of $(R'O)_3Si$-R-$Si(OR')_3$ in an undiluted form and the composition of the materials corresponds to RSi_2O_3. As a result, the materials are very homogeneous. Furthermore, due to the bridging mode of the organic group, it does not protrude into the pore-volume anymore, but is imbedded inside the pore surface. In the meantime a large variety of new and highly interesting PMO materials have been reported. A more comprehensive description can be found in recent review articles.[27] To bring any desired functional group to the surfaces, the corresponding silsesquioxane precursors need to be synthesised first. Therefore, it is challenging to develop multifunctional precursors that can be transformed into a variety of functional entities at the precursor state or even directly at the surfaces of the mesoporous solid. Nice examples for such a multifunctional system are PMOs with bridging ethylene, methylene or bro-

mophenylene and the corresponding precursors.[25,28,29] Ethylene-bridged silica can react in bromination or Diels–Alder reactions.[23,25] In our group we were able to achieve the enantioselective, catalytic hydroboration of bis(trimethoxysilyl)ethene followed by the preparation of a PMO materials with chiral OH groups along the pore surfaces.[30] Another interesting system are PMO materials with bridging Si-CH_2-Si units.[28,31] Earlier, though not on PMO-materials, Corriu showed that the precursor bis(triethoxysilyl)methane can be deprotonated due to the negative hyperconjugation of the molecular orbitals of the two C–H bonds with the antibonding σ* orbitals at the silicon atom. The resulting anion can react with a variety of electrophiles according to nucleophilic substitution reactions.[32]

In our group, we concentrated on a different system containing a phenyl ring as a multifunctional entity.[33] PMO materials with bridging phenyl located along the pore surfaces are very interesting, because it is possible to achieve crystalline pore walls.[34] While all other ordered mesoporous silica and organosilica materials are amorphous, π–π interactions between the phenyl rings can induce local ordering. Furthermore, the thermal stability of the materials is very high; under inert conditions they can be heated up to ≈500 °C and in the presence of oxygen up to ≈380–400 °C without degradation. Further derivatisation of the phenyl ring has also been reported, for example, sulfonation, amination, and conversion to amine-functionalised silica or the attachment organometallic complexes [-$C_6H_4M(CO)_3$-].[35] We became interested in the development of a system of even greater chemical versatility, namely a PMO precursor and resulting mesoporous material containing a bridging bromophenyl entity (see Figure 1).[29] From 1,5-bis(triisopropoxysilyl)-3-bromobenzene it is possible to synthesise a mesoporous organosilica material though not with a highly ordered pore system. The advantage of this system is that the entire range of derivatisation chemistry known for halogenated aromatic compounds can now be applied in the field of PMOs. Different functional groups can be attached to the precursor or alternatively directly in the preformed pore (Figure 1).[29] To date, porous matrices containing benzoic-acid, aninilin, ketones, chiral benzylalcohols or even styrene can be provided with this approach.[36] Because each of these building blocks can be further modified, it is possible to design the functional properties of the mesoporous materials and their surfaces.

Pore-Size Adjustment

One blemish of the chemistry involved in the preparation of mesoporous materials was that most of the obtained silica structures were not discovered by planning, but more by serendipity. Significant work has been devoted to gain more control over the pore shape and size. There is, in principle,

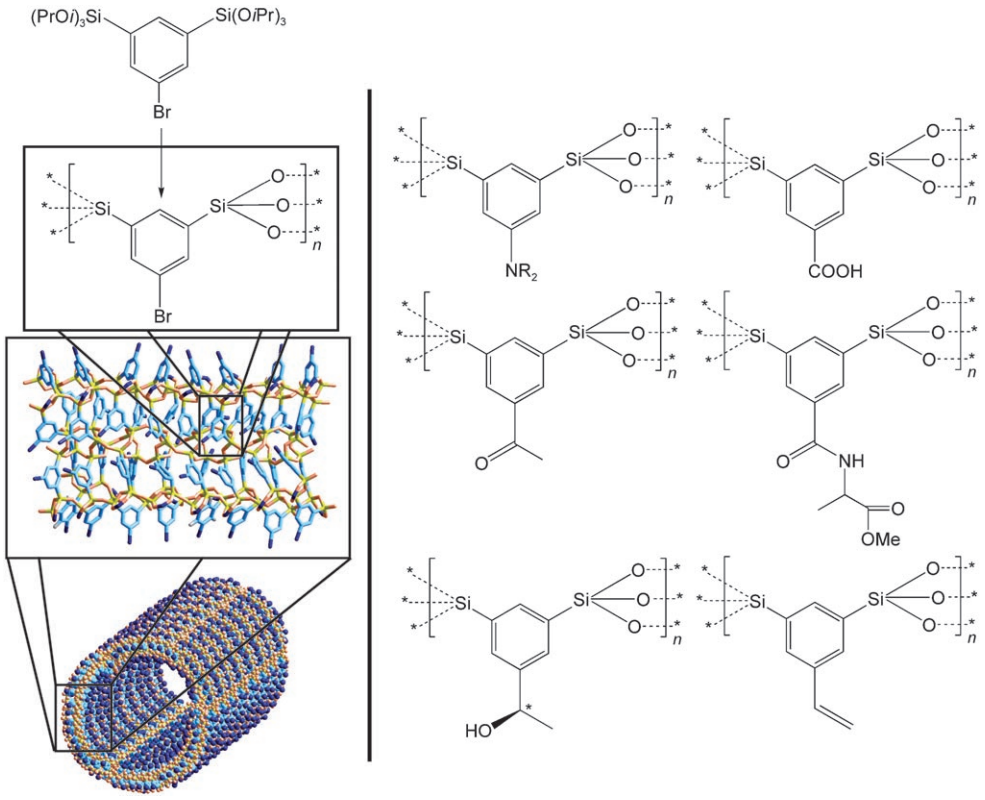

Figure 1. Left-hand side: The formation of a new PMO material from the multifunctional precursor 1,5-bis(triisopropoxysilyl)-3-bromobenzene is shown. The organisation of the bridging organic groups in an amorphous silicate network determined by force-field calculations is indicated. Right-hand side: The variety of PMO materials that can be prepared starting from 1,5-bis(triisopropoxysilyl)-3-bromobenzene as a precursor is shown.

no limitation for accessible pore sizes in amorphous silica materials.[37] The amorphous silica in materials like MCM-41 is insignificantly less stable than the most stable form of SiO_2, crystalline quartz. This means that if a suitable experimental path can be found to reach a certain pore size, then the materials will be absolutely stable. Considering the remarks made about the synthesis of mesoporous materials, it is straightforward to expect that the size of the template will directly influence the size of pores. Consequently, three independent methods exist for pore-size adjustment:

1) The variation of the amphiphile size (especially the hydrophobic part). As larger amphiphilic molecules will lead to larger self-assembled structures (lyotropic phases with larger periodicities) there should be a correlation to pore size.
2) Swelling of the lyotropic phase by addition of selective solvents.
3) Change in reaction parameters like temperature or electrolyte concentration.[38]

All these methods include changes in the packing parameter (N_s) of the amphiphile given in Equation (3), in which v = volume of the hydrophobic chain; l = length of the hydrophobic chain and a_0 = effective area of the head group.

$$N_s = \frac{v}{l a_0} \tag{3}$$

One way to change pore sizes is to vary the temperature during the preparation of the material;[11,39] the higher the temperature, the larger the pores. Also the electrolyte concentration is an important factor.[38] A change in the electrolyte concentration changes the physical character of the aqueous phase and due to interactions of the ions with the ionic/polar head of the surfactant the head-group area. Swelling of the lyotropic phase changes the volume of the hydrophobic chain, which also is included in the packing parameter. Consequently, this can be used for pore-size expansion.[40,41] The dependence of the pore size on the length of ammonia-based surfactants was demonstrated by the first by Beck, Vartuli, Kresge et al.[9,10,42]

An investigation in our group on Brij surfactants $C_x(EO)_y$ showed that this dependency also applies to non-ionic templates, but that in this case the length of the hydrophilic chain influences the pore size as well.[43] A quantitative relation between the size of the mesopore D_c and the composition of the used block copolymer (length of hydrophobic and hydrophilic block) was derived. It was shown that the size of a pore depends, in principle, just on the average number of monomer units in the self-assembled amphiphile structure.[43] This average number can be simply varied if one uses mixtures of amphiphiles (for instance a small and a large surfactant) in different amounts. Besides the prediction of pore sizes from the molecular composition, this is a key-result as it is now possible to obtain every pore size between two borders determined by the "parent templates". The use of liquid crystals of different non-ionic amphiphiles ranging from cyclodextrins,[44] alkyl-poly(ethylene oxide) surfactants, poly(styrene)-poly(ethylene oxide) block copolymers, to poly(ethylene oxide)-poly(propylene oxide)-poly(ethylene oxide) triblock copolymers allows the preparation of mesoporous materials with pore sizes ranging from 1.5 nm to ≈10 nm (see Figure 2c).[43,45] Other groups could even prepare porous materials with pores ≈20 nm in diameter.[46] The mentioned range of pore sizes correlates to confining volumes of several orders of magnitude as indicated in Figure 2b.

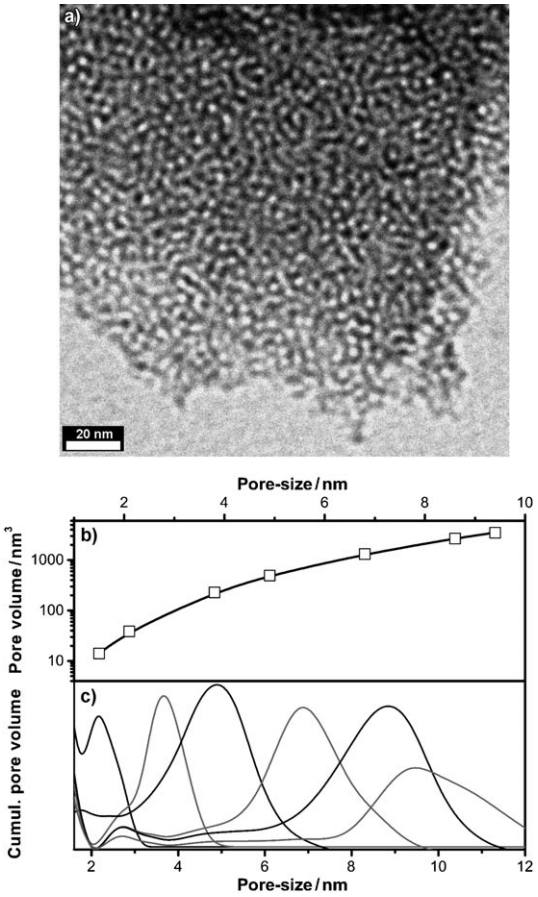

Figure 2. a) A representative TEM image of a mesoporous silica material with a "wormhole" pore system. b) The range of accessible pore volumes. c) DFT Pore-size distribution functions (cumulative pore-volumes) obtained by N_2 physisorption measurements.

Pore Shapes

The pore shape appears to be of minor importance from the viewpoint of molecular reactions occurring under spatial confinement. It is not clear if a reaction is affected by CRFs with same volume but different shapes. However, the situation changes when solid-phases are produced inside the pores of a mesoporous material, because here the shape of the resulting particles often resembles the size and morphology of the pores. Good examples are the synthesis of nano-

wires in cylindrical pores or the replication of the entire pore system by carbon.[47] The pore shape, which is also related to pore connectivity (criterion IV; Scheme 2) is also very important in catalytic applications of porous materials. In catalysis, 3D pore systems possess advantages due to the better mass transport of reactants and products. Like the pore size, the pore shape is also directly connected to the morphology of the intermediate organic–inorganic lyotropic phase. The morphology of a liquid-crystalline phase is mainly concentration-dependent. At first, at low amphiphile concentrations micelles are formed. As the amphiphile concentration increases, more micelles are present that, due to their monodisperse size, pack into ordered arrays of different symmetry. The use of micelles as templates leads to isolated, spherical pores randomly distributed in the silica matrix. Depending on the density of the surrounding matrix it might be impossible to remove the template and to access the pores. The templating of ordered arrays of spherical micelles leads to spherical pores that are eventually connected at the points at which the micelles touch (Figure 3c).[48] Depending on the symmetry and the extend of micelle fusion, different kinds of pores in the form of supercages and 3D pore systems can be generated.[49]

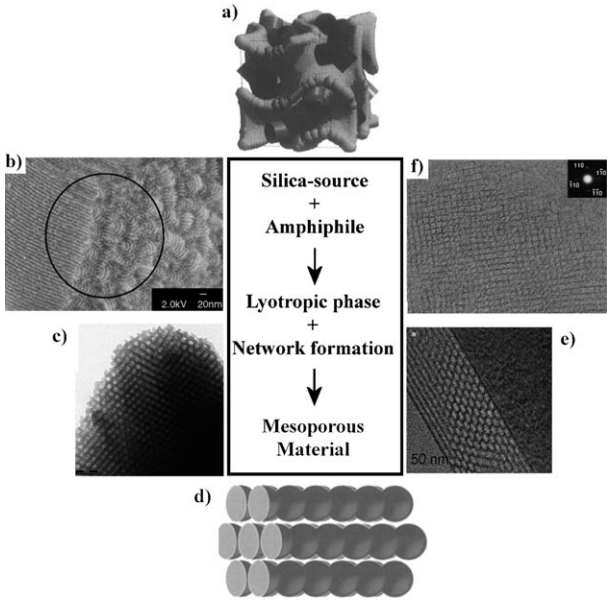

Figure 3. Alternative pore shapes of silica materials. a) Gyroid phase in MCM-48 (schematical image). Reprinted with permission from *Chem. Mater.* **1996**, *8*, 1141. Copyright 1996, American Chemical Society. b) Cylindrical, hexagonally aligned pores observed by SEM. Reprinted with permission from *Angew. Chem.* **2003**, *115*, 2232; *Angew. Chem. Int. Ed.* **2003**, *42*, 2182 . Copyright 2003 Wiley-VCH. c) TEM-image of spherical pores, densely packed. Reprinted with permission from *Langmuir* **2003**, *19*, 4455. Copyright 2003, American Chemical Society. d) Pores with buckled cylinder morphology (schematical image). Reprinted with permission from *Langmuir* **2000**, *16*, 8291. Copyright 2000, American Chemical Society. e) TEM image of rectangular pores, Reprinted with permission from *Non-Cryst. Solids* **2005**, *351*, 2217. Copyright 2005 Elsevier. f) TEM image of rectangular pores, Reprinted with permission from *Angew. Chem.* **2000**, *112*, 4013; *Angew. Chem. Int. Ed.* **2000**, *39*, 3855. Copyright 2000 Wiley-VCH

At higher concentrations of amphiphiles, lyotropic phases form with hexagonal symmetry containing cylindrical aggregates. The use of the such structures as templates leads to the formation of the well-known cylindrical pores reported for MCM-41 or SBA-15 (Figure 3b).[9–11] Due to differences in the formation of mesoporous materials prepared according to the true liquid-crystal-templating and synergistic coassembly mechanisms, pores with a honeycomb cross-section have been reported for MCM-41.[1,13,50] At higher amphiphile concentrations one typically finds lamellar structures, and their use as templates should lead to 2D pores. However, the resulting materials are only stable as long as the template is not removed.[9,10] In the transition region between the cylindrical and lamellar phase, another highly interesting pore structure is possible, the so-called minimal gyroid shape (Figure 3a).[51,52] The addition of swelling agents during the synthesis of the mesoporous silica material can either lead to a pore-size expansion (see previous paragraph) or it can change the morphology of the template more or less dramatically. A nice example is the template transition from a hexagonal, cylindrical shape, through buckled cylinders to an emulsion system caused by the successive addition of trimethylbenzene to a lyotropic crystal of a Pluronic block copolymer as a template (Figure 3d).[40] Interesting effects can occur when the mesoporous material is prepared as a thin film.[53,54] From a cylindrical phase the pores can be contracted in such a way that an elliptical or rectangular cross section results (Figure 3e).[55,56] When Kanemite is used for the synthesis instead of the liquid silica source, interestingly, mesoporous materials with square channels could be obtained (Figure 3f).[57]

Macroscopic Form

The first ordered mesoporous materials were prepared in the form of powders that were precipitated from diluted solutions.[9–12] The single mesoporous particles were typically sized in the sub-micrometer domain and exhibited very unusual shapes.[59] Due to their high potential in diverse applications a lot of research was devoted to the development of mesoporous silica spheres. In the meantime, such materials are available with sphere sizes ranging from several tenth of nanometers to $\approx$1 mm, most of them synthesised by a modified Stoeber process.[60] Mesoporous silica materials with 1D[61] and 2D extensions,[54] that is, fibres and films, respectively, have also extensively studied. However, from the viewpoint of performing chemistry under confined conditions such shapes of mesoporous materials are not absolutely suitable as CRFs. On the one hand it is preferable to have a high number of confined processes happening at the same time, on the other hand you have to make sure that these processes take place exclusively inside the pores and not in the volume between mesoporous particles. A macroscopic block, a so-called monolith, containing only the desired mesoporous system and no additional porosity would be ideally suited as a CRF. Although various reports on

monoliths have been published, it is difficult to prepare a porous monolith with the mentioned characteristics.[62,63] It is feasible to prepare a monolith with filled pores (with solvent or template). A problem is to acquire empty pores. The difficulties are not solely associated with an ordered pore system, although here the template has to be removed prior to drying. The same problems are encountered during the synthesis of aerogels.[21] The problems are connected to the interplay of increasing stiffness of the silica network during condensation and the capillary stress created during drying. At a certain point in the wet state, the silica matrix is not flexible enough for deformation caused by the capillary stress, but also not strong enough to avoid cracks. Therefore, the monolith morphology can normally not be retained under conditions of normal drying. Supercritical drying is required to obtain an ordered mesoporous monolith possessing accessible pores after template removal by liquid–liquid extraction and solvent exchange. On the other hand, granular monolithic silica materials have been reported by careful calcination (see Figure 4).[63,64] The disadvantage of such materials is that they possess only irregular shapes and some cracks. However, the intrapore volume is much larger than the external pore volume. Therefore, this last material fulfils the criterion V indicated in Scheme 2.

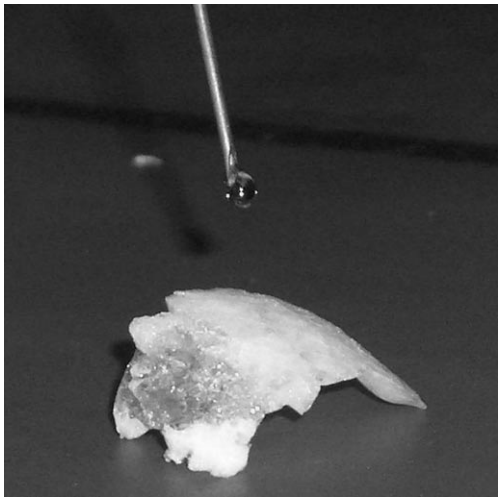

Figure 4. Photographic image of the infiltration of a granular, mesoporous silica monolith prepared by mild calcination with a liquid reactant solution.

Features of chemical processes in CRFs

Influence on chemical equilibria: Considering basic thermodynamic rules, it is evident that many physicochemical processes will be affected by confinements. For instance, a CRF can be regarded as a capillary with very small diameter. The imposed curvature of a liquid meniscus in capillaries gives rise to a Laplace pressure and consequently to a change in vapour pressure of the confined liquid. Typically, the vapour pressure of the liquid decreases with decreasing pore size. The correlation between pore size and vapour pressure is based on Kelvin equation, which in a modified form is used to determine pore-size distributions from physisorption measurements.[65] It is much less evident that also other phase transitions like freezing and melting or phase separations are influenced by spatial confinements.[66,67] However, it was found for numerous systems that the melting point decreases up to $\Delta T = 70\,\mathrm{K}$ depending on the confinement strength.[66,68] It has to be noted that also melting-point depression is a surface effect. Such surface effects are all characterised by the same scaling law typical for the so-called surface dispersion (F) and the fraction of atoms located at the surface: $F \propto N^{-1/3} \propto r^{-1}$ in which N = number of atoms; r = particle radius.[69] The function of the spatial confinement is here to set an upper limit for the particle size $2r$ and to introduce a new type of interface excess energy (wall-solid γ_{ws} and wall-liquid γ_{wf}; see also level I, Scheme 2). The first aspect has been clearly shown even for inorganic nanoparticles growing in confinement.[45,63] Due to quantum size effects, these particles may have special properties, for instance in catalysis.[70] Melting-point depression ΔT can described by the Gibbs–Thomson Equation [Eq. (4)] in which V_m = molar volume and ΔH_m = melting enthalpy.

$$\Delta T = -2\frac{(\gamma_{ws} - \gamma_{wf})V_m}{r\Delta H_m} \tag{4}$$

Considering the Gibbs–Thomson equation, a positive value for ΔT is possible if $\gamma_{ws} < \gamma_{wf}$, that is, if the attractive interaction between the pore surface and the solid phase is stronger than with the liquid phase. However, there are other confinement effects than solely changes in temperature that are possible for phase transitions. The temperature range in which the phase transition occurs can broaden significantly.[71] The reason is that phase transitions are cooperative processes whilst the ensemble inside a CRF is very small.[72]

Such a small ensemble situation can also influence the crystallisation process directly. In some cases alternative crystal phases, amorphous, glassy or even supercooled liquid states for otherwise crystalline materials have been reported in CRFs.[73] A well-studied example is the crystallisation of water in nanoporous silica materials. Here, co-existing ice phases, that is, cubic and hexagonal, can be found.[74] Furthermore, while under standard conditions first-order phase transitions are normal, under spatial confinement the situation can be more complicated. One possibility is a crystal-to-hexatic phase transition prior to liquidification, which means the melting of a crystal occurs in two-dimensions.[75] A small ensemble situation can also influence other chemical processes, which we would like to discuss in some detail in the following paragraphs. Molecular equilibrium reactions are of great interest for the investigation of confinement effects especially when they exhibit more than one possible reaction path. A simple reaction of reactant A with reactant B in equilibrium with a product C is considered in Scheme 3. The number of potential reaction partners B that species A might meet performing a random walk through

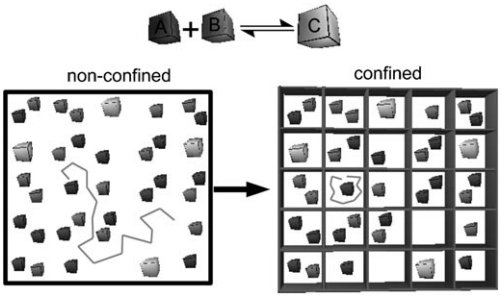

Scheme 3. Confined versus non-confined reaction. Note that neither the distribution nor the density of reactants has been changed on the right-hand side. The grey line indicates a potential random-walk through the system.

the volume is much higher under non-confined conditions in comparison to the confined situation. Although the overall concentration and distribution of molecules has not been changed, the chance for finding a reaction partner has decreased.

The first reaction of the described type that we were investigating concerning the influence of a confining situation was the formation of pyrene excimers.[76] Pyrene is a tetracyclic aromatic molecule (see Figure 5a) that can be excited by light. The resulting excited pyrene can either relax by fluorescence associated with three, well-defined fluorescence signals I–III (see Figure 5b), or it can bind to an additional, ground-state pyrene molecule forming the so-called excimer complex (Figure 5a). The equilibrium between the monomeric pyrenes and the dimeric excimer complex can be expressed by the quotient of the two related fluorescence signals. To obtain a first impression about the role of pyrene–silica interactions we investigated a solution of pyrene in different solvents, but of constant concentration. It is seen (Figure 5b) that in the nonpolar solvent heptane, excimer formation is suppressed completely. Under such conditions the pyrene molecules are immobilised due to adsorption at the SiO_2 walls; this demonstrates the pivotal importance of guest–wall interactions in CRFs. Excimer formation is simply suppressed by immobilisation, but not due to a confinement effect. The adhesion of pyrene on the silica walls can be prohibited when a solvent with similar polarity to the silica surface (like butanol) is used.[77] Solutions of pyrene in butanol with different concentrations have been infiltrated into mesoporous silica materials possessing different pore sizes. The fluorescence measurements were referenced to non-confined solutions of pyrene in butanol.

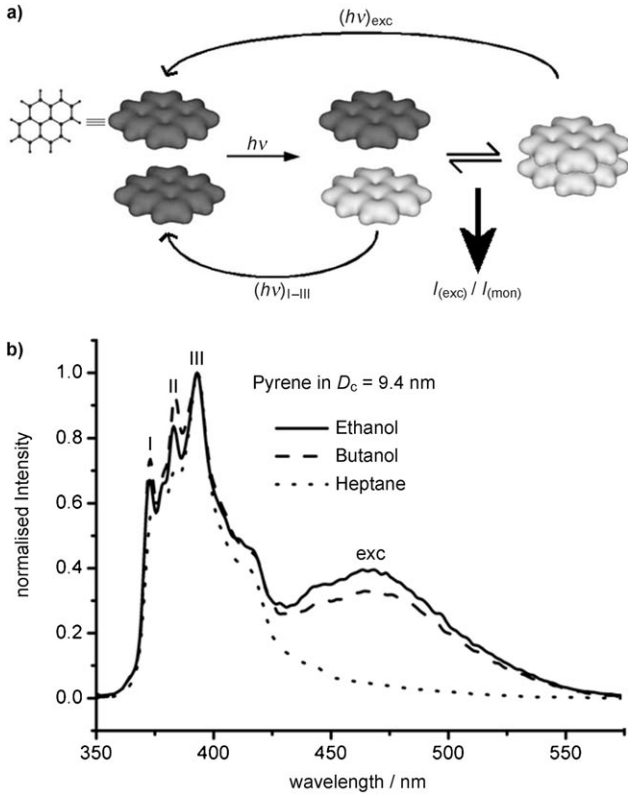

Figure 5. a) Scheme for the formation of pyrene excimers and the associated equilibrium. The light colour indicates that pyrene is in the excited state. b) The fluorescence spectra for solutions of pyrene at a concentration of $c = 6 \times 10^{-3}$ mol L^{-1} in different solvents, infiltrated into a large pore silica-material.

In all cases it is seen that the excimer signal is significantly lower after infiltration (see Figure 5b). Furthermore, the smaller the pores get, the smaller the value for the "equilibrium coefficient" $I_{(exc)}/I_{(mon)}$ (exc = excimer, mon = momer) becomes and the more the equilibrium is shifted to the side of the monomeric species. To understand this effect in more detail, it should be noted that the average number of pyrene molecules N_{pore} is given by the average pore volume and the pyrene concentration [see Eq. (2)]. A plot of $I_{(exc)}/I_{(mon)}$ against N_{pore} is shown in Figure 6a. It is seen that all the experimental points lie on one curve, despite the fact that different materials with different pore sizes have been used. The curve can be described by the following model: How high is the probability for accidently finding two pyrene molecules in one pore, provided that the pyrene molecules at a particular concentration are randomly allocated into a large number of pores? The answer is the Poisson distribution function also shown in Figure 6a. This result indicates that in CRFs the pyrene equilibrium is dictated solely by statistic factors, by the coincidental number of pyrene molecules per pore. Interestingly, this has notable implications beyond the partial suppression of excimer formation.

It is possible to determine thermodynamic parameters for the pyrene–excimer system (ΔG_{exc}, ΔH_{exc}, and ΔS_{exc}) by using methods described in the literature by Stevens and Ban.[78] The enthalpy ΔH_{exc} was calculated by a plot of ln($I_{exc/III}$) against T^{-1} (see Figure 6b). Then, ΔS_{exc} was determined. The difference between the enthalpies for excimer formation for the non-confined in comparison to the confined situation seems to depend linearly on the CRF diameter (Figure 6b). For large pores above 9 nm there is only a small difference to the value expected for the non-confined situation. However, in very small pores the value for ΔH_{exc} differs significantly. The fact that ΔH_{exc} does not scale with the surface dispersion ($\propto r^{-1}$) is a clear indication that the

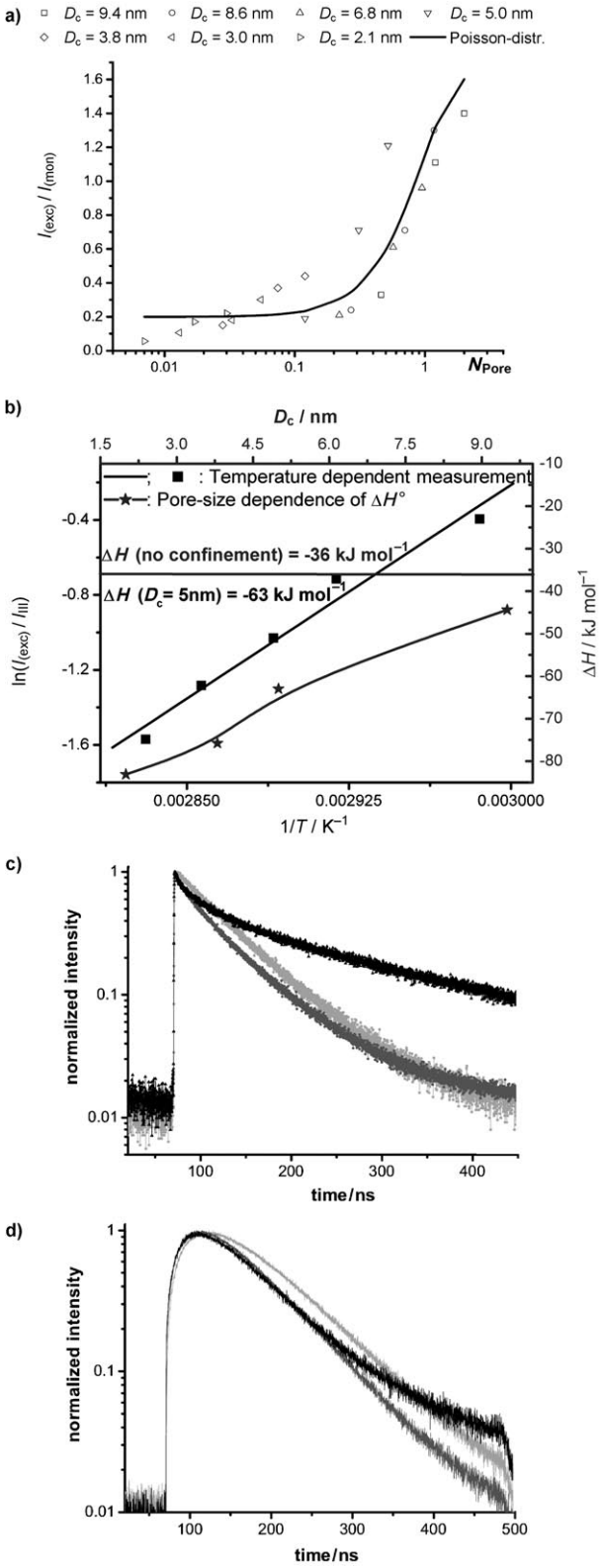

Figure 6. a) The dependence of the relative flourescence intensity $I_{(exc)}/I_{(mon)}$ on the average number of pyrene molecules per pore (N_{pore}). b) The Stevens and Bahn plot for one pore size (black), and the dependence of the reaction enthalpy on pore size (grey). Life-time measurements of pyrene monomers (c) and the excimers (d) under different confinement conditions; no confinement (light grey), medium confinement (grey; $D_{CRF}=8$ nm) and strong confinement (black; $D_{CRF}=2$ nm).

observed effects are caused by the restricted volume. Calculating the entropy for this process from the intercept in Figure 6b, an apparent change from $\Delta S_{exc}=-37\,J\,K^{-1}mol^{-1}$ for the normal solution to $\Delta S_{exc}=-205\,J\,K^{-1}mol^{-1}$ for a 5.0 nm confinement is found. In Figure 6a we can see that the probability for excimer formation is altered due to the confinement to the porous host. From this perspective, and taking into consideration that the equilibrium is shifted towards less excimer formation due to the confinement, it is no longer surprising that the entropy values are also altered. The change of the values of the thermodynamic state functions appears to be strange at first sight, but several points have to be taken into account. It was shown that in the current situation we are dealing with a very small ensemble of pyrene molecules (Figure 6a). A classical thermodynamic treatment does not account for this situation. On other small ensemble systems the description "break-down of thermodynamics" has been used.[72] However, the situation in silica mesopores is somewhat similar to the microcanonical ensemble situation, which is well described in statistical thermodynamics. In the microcanonical ensemble, the entropy depends directly on the probability for a particular microstate p_s [Eq. (5)].

$$S=\sum_{S} p_s \ln p_s \tag{5}$$

Changes in typical equilibrium parameters have also been reported for other systems. It is interesting to note that the enatiomeric excess (*ee*) of a reaction catalysed by a molecular catalyst immobilised at the surfaces of a mesoporous silica host might be pore-size dependent. In the case of an enantioselective, hydrogenation catalyst, the increase in *ee* value was rationalised in such a way that the proximity of the curved surface enhanced the stereospecific induction of the chiral ligand attached to the organometallic Rh complex.[79] However, it should also be considered that spatial confinements might influence the electronic systems of guests directly. For zeolites it is known that such effects are induced on the one hand by strong electrostatic fields,[80] and on the other hand by pure confinement.[81] Although the pore size of MCM-41 is significantly larger than for zeolites, the effect of the confinement on the electronic system of a zinc–phenanthroline complex was reported.[82]

Influence on Kinetics

So far nothing was said about the kinetics of chemical processes in CRFs. It is informative to return to the model system discussed above, pyrene molecules confined to silica mesopores. Lifetime measurements indicate that excited states under confinement relax much slower than in the free system (see Figure 6c,d). The energy once inserted into the system can not be dispersed so easily into Boltzmann distribution. Therefore, it is reasonable that the lifetime of a single pyrene monomer differs very much in different pore

systems (Figure 6c). It can also be seen that a pore size of 8–9 nm imposes practically no significant confinement on the system. Very strong confinements can be found for CRF sizes below 3 nm, which is in agreement with studies performed on other systems.[66,67,83] The longer persistence of excited states can also bee seen on other occasions. If one follows the decomposition of guests located inside silica mesopores using TGA, one frequently finds that the important decomposition steps are shifted towards lower temperatures.[29,45,84] This virtual decrease in activation barrier can be explained by activated states that have a longer lifetime. Thus, a higher probability for the reaction is given in CRFs in comparison to non-confined reference systems. However, one has to be careful with such a simple interpretation. It is more likely to distinguish two cases: 1) that in which there are no appropriate reaction partners present in the CRF to react with the excited species and 2) that in which appropriate reaction partners are present. Imagine reactive radical species as key intermediates in a particular chemical reaction. In silica pores, in the absence of suitable reaction partners, the stability of the radicals is much higher, also because they cannot recombine with other radicals. There were several reports describing the enhanced stability of radicals in silica mesopores studied by EPR spectroscopy, for instance during polymerisation reactions,[85] on surface-confined ketyl radicals[86] and during photoinduced charge separation.[87] However, in the opposite case, if suitable reaction partners are present, the chances for a reaction of these partners are greatly enhanced inside a CRF. This last type of behaviour was demonstrated in a very elegant study in 2005; HO$^{\bullet}$ radicals were generated by radiolysis and were then trapped by the profluorescent compound coumarin.[88] The reaction with coumarin competes with the reaction of hydroxyl radicals with each other and the reaction of hydroxyl radicals with the pore-surface silanol groups. The authors were able to show that under the described conditions there is a significant enhancement for the reaction of the radicals.[88]

Furthermore, the acceleration of chemical reactions plays only a role as long as diffusion through the pore system does not become the dominant factor. It was already mentioned in a previous paragraph that diffusion into the pore system and outside from the pore system in the case of porous materials is unavoidable to fill and empty the pores. Several studies on mobility of guests inside porous materials support the assumption that the diffusion coefficients in CRFs can be significantly smaller.[89] The translational motion of water in MCM-41 was studied by neutron-scattering techniques.[90] Interesting results have been obtained. Not only was the mobility significantly reduced in the CRF, the diffusion showed an Arrhenius type of temperature dependence, unlike bulk water.[90,91] An impressive study on diffusion in mesoporous hosts was presented by Bein et al.[92] The authors were able to identify specific regions of a thin mesoporous film, because they were marked with polystyrene spheres and gold colloids. As a result the movement of single-molecule probes could be followed by fluorescence microscopy mapping, which was then correlated with the pore structure known from TEM measurements recorded at the same position. The authors proved that the shape of the pores determines the mobility of the guests.[92] The movement was unidirectional in cylindrical channels. Furthermore, detailed statements were made about the change in dynamic properties at defects in the porous framework.

Reduced diffusion not only makes the reaction slower, it can also change the reaction order. To study the influence of CRFs on kinetics experimentally, we used mesoporous silica materials possessing different pore sizes and loaded them with molybdenum trioxide (MoO_3).[93] The reduction of the MoO_3 was achieved by the infiltration of an aqueous solution of hydrazinium sulfate. This allowed us to monitor the reaction by UV/Vis and EPR spectroscopy because Mo^{v} is blue and paramagnetic (d^1 system). At high concentrations of hydrazinium salt, the reaction rate can be expressed as Equation (6) in which $\chi(Mo^{VI})$ is the mole-fraction of the Mo^{VI} centres.

$$\frac{d\chi(Mo^{VI})}{dt} = -k'\chi(Mo^{VI})^n \qquad (6)$$

A plot of $\ln(\chi(Mo^{VI}))$ against the time t is informative regarding the order of the reaction n. The corresponding plot is shown in Figure 7 for a mesoporous silica material with small pores (strong confinement) and a material with large pores (weaker confinement). The relationship $\ln(\chi(Mo^{VI}))$ against time is almost linear for strong confinement conditions, indicating a first-order kinetic. Under weak confinement, the reaction is much more complex and practically identical to the non-confined state. The strong impact on kinetics was also verified by Monte-Carlo simulations on general reactions of the type reactant A + reactant B.[94] In rare cases the two confinement effects (acceleration and reaction rate reduction) interfere with each other and a maximum at medium pore sizes is realised. An example is the activity of a surface-bound 1-phospha-3,6-diphenyl-4,5-dimethyl-2-tri-

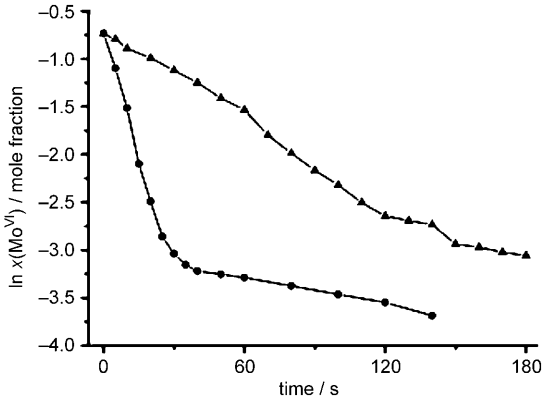

Figure 7. Kinetic plots for the reduction of MoO_3-confined mesoporous silica materials with different pore sizes ($D_p \approx 2$ nm (triangles), $D_p \approx 5$ nm (squares)).[93]

ethoxysilylnorbornadienerhodium(I) complex; the hydrogenation reaction of post-functionalised 1-hexene reached a maximum at intermediate pore sizes of ≈5 nm.[95]

Conclusion

The investigation of chemical processes composed of a small ensemble of reactants is very interesting and delivers some surprising results; different methods exist to obtain such ensembles. Among them, the approach to divide a macroscopic volume into nanoscaled compartments by using porous, inorganic materials appears to be very promising. One of the many advantages of solid, inorganic, porous materials is that they can be operated as CRFs with practically every solvent, and in a very wide temperature (≈550°C for normal silica materials) and pressure range. It was demonstrated that is possible to adjust the properties of porous inorganic solids on various length scales. In the meantime it is possible to modify the surfaces of such materials in such a way that the interaction with guests inside the pores can be adjusted precisely. Here the target-oriented synthesis of mesoporous organosilica materials is of particular importance. Porous materials with narrow pore-size distributions can be produced in the pore-size range of ≈2–20 nm with suitable lyotropic phases as templates. Different pore shapes have been reported, and the materials can be obtained with different macroscopic morphology. Ultimately, monolithic materials are accessible, macroscopic objects avoiding undesired volumes other than the pore volume. The field of OMMs has evidently reached a very high level. However, it seems that the developments highlighted in the current paper regarding surface modification, pore sizes, pore shapes and macroscopic appearance are viewed separately from one another. From the viewpoint of CRFs, a remaining, major challenge is to bring all these features together.

It could be shown that chemistry in confining reaction fields is indeed different from the respective, non-confined cases. Some general trends can be concluded. Matter inside a CRF is automatically forced into a state in which the ratio of surface species to volume becomes a dominating factor. This and the additional interactions with the surfaces of the pore walls lead to a significant change in basic processes determined by thermodynamics, for example, all different kinds of phase-transitions. Even when surface effects do not play a dominant role, CRFs influence equilibrium processes whenever intra- and intermolecular pathways compete. It seems that the statistical number of reactants per CRF (N_{CRF}) determines the chemical behaviour. When $N_{CRF} < 2$, intermolecular reactions are repelled. As a consequence of this it is found that excited states possess a longer lifetime in comparison to non-confined conditions. On the other hand, for $N_{CRF} > 2$ it can even come to an enhancement of the product of the intermolecular process. Furthermore, diffusion in porous matrices is hindered. The restricted mobility of reactants in CRFs can alter the kinetics of chemical processes.

Summarising, one can say that the interaction of guests with the CRF wall is of pivotal importance, and that a CRF diameter of ≈2–5 nm is very effective. Weak confinement is realised in CRFs with diameter 4–7 nm. Above this size confinement effects are only of minor importance.

Acknowledgement

The Deutsche Forschungsgemeinschaft (DFG) is gratefully acknowledged for funding (Emmy-Noether scholarship).

[1] S. Polarz, B. Smarsly, *J. Nanosci. Nanotechnol.* **2003**, *2*, 581.
[2] M. C. Sacchi, D. Zucchi, I. Tritto, P. Locatelli, T. Dallocco, *Macromol. Rapid Commun.* **1995**, *16*, 581; J. C. W. Chien, *Top. Catal.* **1999**, *7*, 23; T. Maschmeyer, F. Rey, G. Sankar, J. M. Thomas, *Nature* **1995**, *378*, 159; R. Anwander, *Chem. Mater.* **2001**, *13*, 4419; F. Silveira, C. F. Petry, D. Pozebon, S. B. Pergher, C. Detoni, F. C. Stedile, J. H. Z. dos Santos, *Appl. Catal. A* **2007**, *333*, 96.
[3] A. Corma, *Chem. Rev.* **1995**, *95*, 559; B. C. Gates, *Chem. Rev.* **1995**, *95*, 511; C. R. Henry, *Surf. Sci. Rep.* **1998**, *31*, 235; N. Mizuno, M. Misono, *Chem. Rev.* **1998**, *98*, 199; D. E. De Vos, M. Dams, B. F. Sels, P. A. Jacobs, *Chem. Rev.* **2002**, *102*, 3615.
[4] A. Corma, *Chem. Rev.* **1997**, *97*, 2373; A. Taguchi, F. Schuth, *Microporous Mesoporous Mater.* **2005**, *77*, 1.
[5] K. S. W. Sing, D. H. Everett, R. A. W. Haul, L. Moscou, R. A. Pierotti, J. Rouquérol, T. Siemieniewska, *Pure Appl. Chem.* **1985**, *57*, 603.
[6] D. G. Shchukin, G. B. Sukhorukov, *Adv. Mater.* **2004**, *16*, 671.
[7] Y. Rharbi, N. Bechthold, K. Landfester, A. Salzman, M. A. Winnik, *Langmuir* **2003**, *19*, 10.
[8] J. Y. Ying, C. P. Mehnert, M. S. Wong, *Angew. Chem.* **1999**, *111*, 58; *Angew. Chem. Int. Ed.* **1999**, *38*, 56; U. Ciesla, F. Schüth, *Microporous Mesoporous Mater.* **1999**, *27*, 131.
[9] J. S. Beck, J. C. Vartuli, W. J. Roth, M. E. Leonowicz, C. T. Kresge, K. D. Schmitt, C. T. Chu, D. H. Olson, E. W. Sheppard, S. B. McCullen, J. B. Higgins, J. L. Schlenker, *J. Am. Chem. Soc.* **1992**, *114*, 10834.
[10] C. T. Kresge, M. Leonowicz, W. J. Roth, J. C. Vartuli, J. S. Beck, *Nature* **1992**, *359*, 710.
[11] D. Zhao, J. Feng, Q. Huo, N. Melosh, G. H. Fredrickson, B. F. Chmelka, G. D. Stucky, *Science* **1998**, *279*, 548.
[12] P. Yang, D. Zhao, D. I. Margolese, B. F. Chmelka, G. D. Stucky, *Nature* **1998**, *396*, 152.
[13] S. Polarz, M. Antonietti, *Chem. Commun.* **2002**, 2593.
[14] B. Smarsly, C. Goeltner, M. Antonietti, W. Ruland, E. Hoinkis, *J. Phys. Chem. B* **2001**, *105*, 831; C. G. Goeltner, B. Smarsly, B. Berton, M. Antonietti, *Chem. Mater.* **2001**, *13*, 1617.
[15] H. Landmesser, H. Kosslick, W. Storek, R. Fricke, *Solid State Ionics* **1997**, *101*, 271; X. S. Zhao, G. Q. Lu, A. K. Whittaker, G. J. Millar, H. Y. Zhu, *J. Phys. Chem. B* **1997**, *101*, 6525; M. Widenmeyer, R. Anwander, *Chem. Mater.* **2002**, *14*, 1827.
[16] E. W. Abel, F. H. Pollard, P. C. Uden, G. Nickless, *J. Chromatogr.* **1966**, *22*, 23; R. K. Gilpin, M. F. Burke, *Anal. Chem.* **1973**, *45*, 1383; U. Deschler, P. Kleinschmit, P. Panster, *Angew. Chem.* **1986**, *98*, 237; *Angew. Chem. Int. Ed.* **1986**, *25*, 236.
[17] U. Schubert, N. Huesing, A. Lorenz, *Chem. Mater.* **1995**, *7*, 2010.
[18] S. A. Raynor, J. M. Thomas, R. Raja, B. F. G. Johnson, R. G. Bell, M. D. Mantle, *Chem. Commun.* **2000**, 1925.
[19] D. R. Radu, C. Y. Lai, K. Jeftinija, E. W. Rowe, S. Jeftinija, V. S. Y. Lin, *J. Am. Chem. Soc.* **2004**, *126*, 13216; A. B. Descalzo, D. Jimenez, M. D. Marcos, R. Martinez-Manez, J. Soto, J. El Haskouri, C. Guillem, D. Beltran, P. Amoros, M. V. Borrachero, *Adv. Mater.* **2002**, *14*, 966; A. Matsumoto, K. Tsutsumi, K. Schumacher, K. K. Unger, *Langmuir* **2002**, *18*, 4014.
[20] P. Sutra, D. Brunel, *Chem. Commun.* **1996**, 2485.

[21] N. Hüsing, U. Schubert, *Angew. Chem.* **1998**, *110*, 22; *Angew. Chem. Int. Ed.* **1998**, *37*, 22.
[22] S. L. Burkett, S. D. Sims, S. Mann, *Chem. Commun.* **1996**, 1367; D. J. Macquarrie, *Chem. Commun.* **1996**, 1961.
[23] T. Asefa, M. J. MacLachan, N. Coombs, G. A. Ozin, *Nature* **1999**, *402*, 867.
[24] S. Inagaki, S. Guan, Y. Fukushima, T. Ohsuna, O. Terasaki, *J. Am. Chem. Soc.* **1999**, *121*, 9611.
[25] B. J. Melde, B. T. Holland, C. F. Blanford, A. Stein, *Chem. Mater.* **1999**, *11*, 3302.
[26] K. J. Shea, D. A. Loy, O. Webster, *J. Am. Chem. Soc.* **1992**, *114*, 6700; R. J. P. Corriu, J. J. E. Moreau, P. Thepot, M. W. C. Man, *Chem. Mater.* **1992**, *4*, 1217; D. A. Loy, K. J. Shea, *Chem. Rev.* **1995**, *95*, 1431.
[27] B. Hatton, K. Landskron, W. Whitnall, D. Perovic, G. A. Ozin, *Acc. Chem. Res.* **2005**, *38*, 305; F. Hoffmann, M. Cornelius, J. Morell, M. Froeba, *Angew. Chem.* **2006**, *118*, 3290; *Angew. Chem. Int. Ed.* **2006**, *45*, 3216.
[28] T. Asewa, M. J. MacLachlan, H. Grondey, N. Coombs, G. A. Ozin, *Angew. Chem.* **2000**, *112*, 1878; *Angew. Chem. Int. Ed.* **2000**, *39*, 1808.
[29] A. Kuschel, S. Polarz, *Adv. Funct. Mater.* **2008**, *18*, 1272.
[30] S. Polarz, A. Kuschel, *Adv. Mater.* **2006**, *18*, 1206; A. Ide, R. Voss, G. Scholz, G. A. Ozin, A. Antonietti, A. Thomas, *Chem. Mater.* **2007**, *19*, 2649.
[31] K. Landskron, B. D. Hatton, D. D. Perovic, G. A. Ozin, *Science* **2003**, *302*, 266.
[32] R. J. P. Corriu, M. Granier, G. F. Lanneau, *J. Organomet. Chem.* **1998**, *562*, 79.
[33] C. Yoshina-Ishii, T. Asefa, N. Coombs, M. J. MacLachlan, G. A. Ozin, *Chem. Commun.* **1999**, 2539; S. Guan, S. Inagaki, T. Ohsuna, O. Terasaki, *J. Am. Chem. Soc.* **2000**, *122*, 5660; Y. Goto, S. Inagaki, *Chem. Commun.* **2002**, 2410; Q. H. Yang, M. P. Kapoor, S. Inagaki, *J. Am. Chem. Soc.* **2002**, *124*, 9694; M. P. Kapoor, Q. H. Yang, S. Inagaki, *Chem. Mater.* **2004**, *16*, 1209.
[34] S. Inagaki, S. Guan, T. Ohsuna, O. Terasaki, *Nature* **2002**, *416*, 304.
[35] T. Asefa, M. Kruk, M. J. MacLachlan, N. Coombs, H. Grondey, M. Jaroniec, G. A. Ozin, *J. Am. Chem. Soc.* **2001**, *123*, 8520; T. Kamegawa, T. Sakai, M. Matsuoka, M. Anpo, *J. Am. Chem. Soc.* **2005**, *127*, 16784; M. Ohashi, S. Inagaki, *Chem. Commun.* **2008**, 841.
[36] A. Kuschel, S. Polarz, unpublished results.
[37] A. Navrotsky, I. Petrovic, Y. Hu, C. Chen, M. E. Davies, *J. Non-Cryst. Solids* **1995**, *192–193*, 474.
[38] A. Corma, Q. Kan, M. T. Navarro, J. Pérez-Pariente, F. Rey, *Chem. Mater.* **1997**, *9*, 2123.
[39] E. Prouzet, T. J. Pinnavaia, *Angew. Chem.* **1997**, *109*, 533; *Angew. Chem. Int. Ed. Engl.* **1997**, *36*, 516.
[40] J. S. Lettow, Y. J. Han, P. Schmidt-Winkel, P. Yang, D. Zhao, G. D. Stucky, J. Y. Ying, *Langmuir* **2000**, *16*, 8291.
[41] J. N. Israelachvili, D. J. Mitchell, B. W. Ninham, *J. Chem. Soc. Faraday Trans. 2* **1976**, *72*, 1525; J. Israelachvili, *Intermolecular and Surface Forces*, 2 ed., Academic Press, London, **1991**; D. J. Mitchell, B. W. Ninham, *J. Chem. Soc. Faraday Trans. 2* **1981**, *77*, 601; A. Sayari, Y. Yang, M. Kruk, M. Jaroniec, *J. Phys. Chem. B* **1999**, *103*, 3651; A. Sayari, *Angew. Chem.* **2000**, *112*, 3042; *Angew. Chem. Int. Ed.* **2000**, *39*, 2920.
[42] J. S. Beck, J. C. Vartuli, *Curr. Opin. Colloid Interface Sci.* **1996**, *1*, 76.
[43] B. Smarsly, S. Polarz, M. Antonietti, *J. Phys. Chem. B* **2001**, *105*, 10473.
[44] S. Polarz, B. Smarsly, L. Bronstein, M. Antonietti, *Angew. Chem.* **2001**, *113*, 4549; *Angew. Chem. Int. Ed.* **2001**, *40*, 4417; B. H. Han, S. Polarz, M. Antonietti, *Chem. Mater.* **2001**, *13*, 3915.
[45] S. Polarz, F. Neues, M. Van den Berg, W. Grünert, L. Khodeir, *J. Am. Chem. Soc.* **2005**, *127*, 12028.
[46] A. Thomas, H. Schlaad, B. Smarsly, M. Antonietti, *Langmuir* **2003**, *19*, 4455.
[47] J. Han, J. M. Kim, G. D. Stucky, *Chem. Mater.* **2000**, *12*, 2068; C. H. Ko, R. Ryoo, *Chem. Commun.* **1996**, 2467; R. Ryoo, S. H. Joo, S. Jun, *J. Phys. Chem. B* **1999**, *103*, 7743; R. Ryoo, S. H. Joo, M. Kruk, M. Jaroniec, *Adv. Mater.* **2001**, *13*, 677.
[48] J. M. Kim, Y. Sakamoto, Y. K. Hwang, Y. U. Kwon, O. Terasaki, S. E. Park, G. D. Stucky, *J. Phys. Chem. B* **2002**, *106*, 2552; Q. Huo, R. Leon, P. M. Petroff, G. D. Stucky, *Science* **1995**, *268*, 1324; Q. Huo, D. I. Margolese, G. D. Stucky, *Chem. Mater.* **1996**, *8*, 1147; Y. F. Lu, H. Y. Fan, N. Doke, D. A. Loy, R. A. Assink, D. A. LaVan, C. J. Brinker, *J. Am. Chem. Soc.* **2000**, *122*, 5258.
[49] Q. S. Huo, R. Leon, P. M. Petroff, G. D. Stucky, *Science* **1995**, *268*, 1324; Q. S. Huo, D. I. Margolese, U. Ciesla, P. Y. Feng, T. E. Gier, P. Sieger, R. Leon, P. M. Petroff, F. Schueth, G. D. Stucky, *Nature* **1994**, *368*, 317; Y. Sakamoto, I. Diaz, O. Terasaki, D. Y. Zhao, J. Perez-Pariente, J. M. Kim, G. D. Stucky, *J. Phys. Chem. B* **2002**, *106*, 3118; Y. Sakamoto, M. Kaneda, O. Terasaki, D. Y. Zhao, J. M. Kim, G. Stucky, H. J. Shim, R. Ryoo, *Nature* **2000**, *408*, 449; T.-W. Kim, F. Kleitz, B. Paul, R. Ryooo, *J. Am. Chem. Soc.* **2005**, *127*, 7601; S. A. El-Safty, T. Hanaoka, F. Mizukami, *Chem. Mater.* **2005**, *17*, 3137.
[50] A. Monnier, F. Schüth, Q. Huo, D. Kumar, D. Margolese, R. S. Maxwell, G. D. Stucky, M. Krishnamurty, P. Petroff, A. Firouzi, M. Janicke, B. F. Chmelka, *Science* **1993**, *261*, 1299.
[51] V. Alfredsson, M. W. Anderson, *Chem. Mater.* **1996**, *8*, 1141.
[52] M. W. Anderson, *Zeolites* **1997**, *19*, 220.
[53] C. J. Brinker, Y. F. Lu, A. Sellinger, H. Y. Fan, *Adv. Mater.* **1999**, *11*, 579.
[54] C. Sanchez, C. Boissière, D. Grosso, C. Laberty, L. Nicole, *Chem. Mater.* **2008**, *20*, 682.
[55] D. Grosso, A. R. Balkenende, P. A. Albouy, M. Lavergne, L. Mazerolles, F. Babonneau, *J. Mater. Chem.* **2000**, *10*, 2085; P. Falcaro, D. Grosso, H. Amenitsch, P. Innocenzi, *J. Phys. Chem. B* **2004**, *108*, 10942.
[56] R. E. Williford, R. S. Addleman, X. S. Li, T. S. Zemanian, J. C. Birnbaum, G. E. Fryxell, *J. Non-Cryst. Solids* **2005**, *351*, 2217.
[57] T. Kimura, T. Kamata, M. Fuziwara, Y. Takano, M. Kaneda, Y. Sakamoto, O. Terasaki, Y. Sugahara, K. Kuroda, *Angew. Chem.* **2000**, *112*, 4013; *Angew. Chem. Int. Ed.* **2000**, *39*, 3855.
[58] S. N. Che, K. Lund, T. Tatsumi, S. Iijima, S. H. Joo, R. Ryoo, O. Terasaki, *Angew. Chem.* **2003**, *115*, 2232; *Angew. Chem. Int. Ed.* **2003**, *42*, 2182.
[59] H. Yang, N. Coombs, G. A. Ozin, *Nature* **1997**, *386*, 692; S. M. Yang, I. Sokolov, N. Combs, C. T. Kresge, G. A. Ozin, *Adv. Mater.* **1999**, *11*, 1427; I. Sokolov, H. Yang, G. A. Ozin, C. T. Kresge, *Adv. Mater.* **1999**, *11*, 636; S. M. Yang, H. Yang, N. Coombs, I. Sokolov, C. T. Kresge, G. A. Ozin, *Adv. Mater.* **1999**, *11*, 52; D. Y. Zhao, J. Y. Sun, Q. Z. Li, G. D. Stucky, *Chem. Mater.* **2000**, *12*, 275.
[60] B. G. Trewyn, I. I. Slowing, S. Giri, H.-T. Chen, V. S.-Y. Lin, *Acc. Chem. Res.* **2007**, *40*, 846; H. Yang, G. Vovk, N. Coombs, I. Sokolov, G. A. Ozin, *J. Mater. Chem.* **1998**, *8*, 743; Q. Huo, J. Feng, F. Schüth, G. D. Stucky, *Chem. Mater.* **1997**, *9*, 14; S. Liu, L. Lu, Z. Yang, P. Cool, E. F. Vansant, *Mater. Chem. Phys.* **2006**, *97*, 203; A. Arkhireeva, J. N. Hay, *J. Mater. Chem.* **2003**, *13*, 3122; D. Y. Zhao, P. D. Yang, Q. S. Huo, B. F. Chmelka, G. D. Stucky, *Curr. Opin. Solid State Mater. Sci.* **1998**, *3*, 111.
[61] F. Kleitz, F. Marlow, G. D. Stucky, F. Schüth, *Chem. Mater.* **2001**, *13*, 3587; P. D. Yang, D. Y. Zhao, B. F. Chmelka, G. D. Stucky, *Chem. Mater.* **1998**, *10*, 2033; P. J. Bruinsma, A. Y. Kim, J. Liu, S. Baskaran, *Chem. Mater.* **1997**, *9*, 2507; Q. S. Huo, D. Y. Zhao, J. L. Feng, K. Weston, S. K. Buratto, G. D. Stucky, S. Schacht, F. Schüth, *Adv. Mater.* **1997**, *9*, 974.
[62] M. C. Weissenberger, C. G. Goeltner, M. Antonietti, *Ber. Bunsen-Ges.* **1997**, *101*, 1679; M. T. Anderson, J. E. Martin, J. G. Odinek, P. P. Newcomer, J. P. Wilcoxon, *Microporous Mater.* **1997**, *10*, 13; S. A. El-Safty, F. Mizukami, T. Hanaoka, *J. Mater. Chem.* **2005**, *15*, 2590; D. Brandhuber, H. Peterlik, N. Huesing, *J. Mater. Chem.* **2005**, *15*, 3896; J. H. Smatt, S. Schunk, M. Linden, *Chem. Mater.* **2003**, *15*, 2354.
[63] L. M. Bronstein, S. Polarz, B. Smarsly, M. Antonietti, *Adv. Mater.* **2001**, *13*, 1333.
[64] Y. Mastai, S. Polarz, M. Antonietti, *Adv. Funct. Mater.* **2002**, *12*, 197.

[65] J. Rouqerol, D. Avnir, C. W. Fairbridge, D. H. Everett, J. H. Haynes, N. Pernicone, J. D. Ramsay, K. S. W. Sing, K. K. Unger, *Pure Appl. Chem.* **1994**, *66*, 1739; S. J. Gregg, K. S. W. Sing, *Adsorption, Surface Area and Porosity, Vol. 2*, 4 ed., Academic Press, **1982**.
[66] L. D. Gelb, K. E. Gubbins, R. Radhakrishnan, M. Sliwinska-Bartowiak, *Rep. Prog. Phys.* **1999**, *62*, 1573.
[67] C. Alba-Simionescu, B. Coasne, G. Dosseh, G. Dudziak, K. E. Gubbins, R. Radhakrishnan, M. Sliwinska-Bartowiak, *J. Phys. Condens. Matter* **2006**, *18*, R15.
[68] H. F. Booth, J. H. Strange, *Mol. Phys.* **1998**, *93*, 263; A. Schreiber, I. Ketelsen, G. H. Findenegg, *Phys. Chem. Chem. Phys.* **2001**, *3*, 1185.
[69] E. Roduner, *Nanoscopic Materials: Size-Dependent Phenomena*, The Royal Society of Chemistry, Cambridge, **2006**.
[70] C. Aprile, A. Corma, H. Garcia, *Phys. Chem. Chem. Phys.* **2008**, *10*, 769.
[71] K. M. Unruh, T. E. Huber, C. A. Huber, *Phys. Rev. B* **1993**, *48*, 9021.
[72] E. Roduner, *Chem. Soc. Rev.* **2006**, *35*, 583.
[73] G. Dosseh, Y. Xia, C. Alba-Simionescu, *J. Phys. Chem. B* **2003**, *107*, 6445.
[74] J. M. Baker, J. C. Dore, P. Behrens, *J. Phys. Chem. B* **1997**, *101*, 6226; J. C. Dore, B. Webber, M. Hartl, P. Behrens, T. Hansen, *Phys. A* **2002**, *314*, 501.
[75] B. I. Halperin, D. R. Nelson, *Phys. Rev. Lett.* **1978**, *41*, 121; F. Bruni, M. A. Ricci, A. K. Sopper, *J. Chem. Phys.* **1998**, *109*, 1478; M. Sliwinska-Bartowiak, G. Dudziak, R. Sikorski, R. Gras, K. E. Gubbins, R. Radhakrishnan, *Phys. Chem. Chem. Phys.* **2001**, *3*, 1179.
[76] T. Foerster, K. Kasper, *Z. Elektrochem.* **1955**, *59*, 976.
[77] A. Thomas, S. Polarz, M. Antonietti, *J. Phys. Chem. B* **2003**, *107*, 5081.
[78] B. Stevens, M. I. Ban, *Transactions of the Faraday Society* **1964**, *60*, 1515; J. B. Birks, *Photophysics of Aromatic Molecules*, Wiley-Interscience, London, **1970**.
[79] M. D. Jones, R. Raja, J. M. Thomas, B. F. G. Johnson, D. W. Lewis, J. Rouzand, K. D. M. Harris, *Angew. Chem.* **2003**, *115*, 4462; *Angew. Chem. Int. Ed.* **2003**, *42*, 4326; R. Raja, J. M. Thomas, M. D. Jones, B. F. G. Johnson, D. E. W. Vaughan, *J. Am. Chem. Soc.* **2003**, *125*, 14982.
[80] F. Blatter, H. Frei, **1993**, *J. Am. Chem. Soc. 115*, 7501; H. Sun, F. Blatter, H. Frei, *J. Am. Chem. Soc.* **1996**, *118*, 6873.
[81] F. Marquez, H. Garcia, E. Palomares, L. Fernandez, A. Corma, *J. Am. Chem. Soc.* **2000**, *122*, 6520.
[82] L. Z. Zhang, P. Cheng, D. Z. Liao, *J. Chem. Phys.* **2002**, *117*, 5959.
[83] F. Goettmann, C. Sanchez, *J. Mater. Chem.* **2007**, *17*, 24.
[84] M. K. Kidder, P. F. Britt, Z. T. Zhang, S. Dai, E. W. Hagaman, A. L. Chaffee, A. C. Buchanan, *J. Am. Chem. Soc.* **2005**, *127*, 6353.
[85] S. M. Ng, S. Ogino, T. Aida, K. A. Koyano, T. Tatsumi, *Macromol. Rapid Commun.* **1997**, *18*, 991.
[86] I. Nagl, M. Widenmeyer, S. Grasser, K. Kohler, R. Anwander, *J. Am. Chem. Soc.* **2000**, *122*, 1544.
[87] V. Kuchi, A. M. Oliver, M. N. Paddon-Row, R. F. Howe, *Chem. Commun.* **1999**, 1149; Y. Kim, J. R. Choi, M. Yoon, A. Furube, T. Asahi, H. Masuhara, *J. Phys. Chem. B* **2001**, *105*, 8513.
[88] S. Foley, P. Rotureau, S. Pin, G. Baldacchino, J. P. Renault, J. C. Mialocq, *Angew. Chem.* **2005**, *117*, 112; *Angew. Chem. Int. Ed.* **2005**, *44*, 110.
[89] J. P. Korb, S. Xu, F. Cros, L. Malier, J. Jonas, *J. Chem. Phys.* **1997**, *107*, 4044; F. Cros, J. P. Korb, L. Malier, *Langmuir* **2000**, *16*, 10193.
[90] S. Takahara, M. Nakano, S. Kittaka, Y. Kuroda, T. Mori, H. Hamano, T. Yamaguchi, *J. Phys. Chem. B* **1999**, *103*, 5814.
[91] J. Karger, D. Freude, *Chem. Eng. Technol.* **2002**, *25*, 769.
[92] J. Kirstein, B. Platschek, C. Jung, R. Brown, T. Bein, C. Brauchle, *Nat. Mater.* **2007**, *6*, 303; A. Zurner, J. Kirstein, M. Doblinger, C. Brauchle, T. Bein, *Nature* **2007**, *450*, 705; C. Jung, J. Kirstein, B. Platschek, T. Bein, M. Budde, I. Frank, K. Muellen, J. Michaelis, C. Braeuchle, **2008**, *130*, 1638.
[93] V. Hornebecq, Y. Mastai, M. Antonietti, S. Polarz, *Chem. Mater.* **2003**, *15*, 3586.
[94] J. Ahn, R. Kopelman, P. Argyrakis, *J. Chem. Phys.* **1999**, *110*, 2116; A. L. Lin, E. Monson, R. Kopelman, *Phys. Rev. E* **1997**, *56*, 1561; A. L. Lin, R. Kopelman, P. Argyrakis, *J. Phys. Chem. A* **1997**, *101*, 802.
[95] F. Goettmann, D. Grosso, F. Mercier, F. Mathey, C. Sanchez, *Chem. Commun.* **2004**, 1240.

Published online: July 24, 2008

